Journal of Pharmaceutical and Biomedical Analysis 185 (2020) 113230

Contents lists available at ScienceDirect

Journal of Pharmaceutical and Biomedical Analysis

journal homepage: www.elsevier.com/locate/jpba

Quantitation of polymeric-microneedle-delivered HA15 in tissues using liquid chromatography-tandem mass spectrometry

Parbeen Singh[a,c,1], Xiliu Zeng[c,1], Xiaowu Chen[f], Yikun Yang[b], Yongli Chen[a,c,*], Shufen Cui[c], Andrew Carrier[d], Ken Oakes[e], Tiangang Luan[a], Xu Zhang[d,**]

[a] State Key Laboratory Biocontrol, School of Marine Sciences, Sun Yat-sen University, Guangzhou, 510275, China
[b] National Cancer Center/National Clinical Research Center for Cancer/Cancer Hospital & Shenzhen Hospital, Chinese Academy of Medical Sciences and Peking Union Medical College, Shenzhen, 518116, China
[c] Department of Biological Applied Engineering, Shenzhen Key Laboratory of Fermentation Purification and Analysis, Shenzhen Polytechnic, Shenzhen, 518055, China
[d] Department of Chemistry, 1250 Grand Lake Road, Sydney, Nova Scotia, B1P 6L2, Canada
[e] Department of Biology, Cape Breton University, 1250 Grand Lake Road, Sydney, Nova Scotia, B1P 6L2, Canada
[f] Shenzhen Kivita Innovative Drug Discovery Institute, Shenzhen, 518110, China

ARTICLE INFO

Article history:
Received 10 December 2019
Received in revised form 2 March 2020
Accepted 3 March 2020
Available online 4 March 2020

Keywords:
Microneedle
Liquid chromatography-tandem mass spectrometry
Drug distribution
HA15

ABSTRACT

A rapid and sensitive liquid chromatography-tandem mass spectrometric method was developed and validated for the determination of HA15, an emerging anticancer compound targeting GSPA5/BIP delivered by dissolvable polymeric microneedles. The linear range of quantification for HA15 was 2.5–1000 ng/ml in plasma and tissue homogenate and the limit of detection and lower limit of quantification are 1 and 2.5 ng/ml, respectively. The inter- and intra-day accuracy and precision were within the acceptable range. HA15 was extracted from mouse plasma and organs using protein precipitation and using dabrafenib as an internal standard and the drug was stable under relevant analytical conditions. The method was used to analyze drug loading, dissolution *in vitro*, and release *ex vivo* from dissolvable polymeric microneedles and used to compare these materials to subcutaneous injection for the tissue distribution in tumor bearing nude mice.

© 2020 Elsevier B.V. All rights reserved.

1. Introduction

HA15 is a new chemotherapeutic compound effective in treating melanoma and adrenocortical carcinoma [1,2]. It targets GSPA5/BIP, which responds to endoplasmic reticulum stress and induces cell death by concomitant induction of autophagy and apoptosis [3]. It is often delivered subcutaneously, *e.g.*, daily injections for two weeks. However, subcutaneous and intravenous administration are painful, pose a risk of infection, produce sharp and bio-hazardous wastes, and may require a healthcare practitioner [4,5]. A new safe, effective, more comfortable, and self-administrable formulation could reduce healthcare costs and improve patient quality of life.

Microneedles (MNs) are arrays of up to 2000 miniaturized needles per cm^2 on a supporting patch that are <1 mm long, which were developed in the 1990s by Prausnitz for use as transdermal drug delivery devices [6–8]. MNs can deliver their therapeutic cargo effectively via penetration of the *stratum corneum* in a painless and minimally invasive manner [9–13]. Dissolvable polymeric MNs (DPMNs) are attractive because they promise scalable production [14], deliver chemical and biological therapeutics, and do not generate waste sharps [15]. In addition, DPMNs allow for controlled drug release in skin for various biomedical applications [16–19]. However, as an innovative and promising approach to transdermal drug delivery, evaluation of their various pharmacokinetic parameters, *e.g.*, their drug loading capacity, permeation efficiency, release kinetics, diffusion within the epidermis and dermis, distribution and metabolism, is critical for pre-clinical and clinical studies. Recently, DPMN-based transdermal drug delivery was compared with conventional subcutaneous injection in pharmacokinetic studies, showing no significant difference between the methods in terms of the area under curve and t_{max} values, indicating the promise of DPMNs for delivery of therapeutics [20,21].

* Corresponding author at: MOE Key Laboratory of Aquatic Product Safety, School of Marine Sciences, Sun Yat-sen University, Guangzhou, 510275, China.
** Corresponding author.
E-mail addresses: chenyongli0617@163.com (Y. Chen), xu_zhang@cbu.ca (X. Zhang).
[1] These authors contributed equally to the work.

https://doi.org/10.1016/j.jpba.2020.113230
0731-7085/© 2020 Elsevier B.V. All rights reserved.

Nevertheless, such quantitative analysis and evaluation of DPMN pharmacokinetics is still limited [22–24].

Herein we developed and validated a simple, sensitive, and specific LC–MS/MS method to quantitatively evaluate HA15 delivery by DPMNs and investigate its tissue distribution through different administration routes. The validation results showed high sensitivity and specificity for HA15 and the method was successfully applied to evaluating DPMN drug loading, *in vitro* drug release kinetics, and HA15 biodistribution after subcutaneous or DPMN administration. This work reports the LC–MS/MS method for HA15 quantification and demonstrates its application for the evaluation of the biodistribution of HA15 delivered by the novel microneedle approach and is thus useful for both pharmaceutical analysis and drug delivery studies.

2. Material and methods

2.1. Materials and reagents

Formic acid was purchased from Sigma-Aldrich (St. Louis, MO, USA). HA15 (Fig. 1A, 99.61 % purity) was obtained from Selleck Chemicals (Houston, TX, USA). Poly (vinylpyrrolidone) (PVP K30, MW = 30,000) was obtained from Sangon Biotech (Shanghai, China). Poly (vinyl alcohol) (PVA, 88 % hydrolyzed, 4.5–6.0 mPa s) and dabrafenib (the internal standard, IS, Fig. 1B, 98 % purity) were obtained from J&K Chemical Co. Ltd. (Beijing, China). Human melanoma cell line B16F10 was obtained from the China Infrastructure of Cell Line Resource (Beijing, China). Fetal bovine serum (FBS) and cell culture media were obtained from Invitrogen Life Technologies (Carlsbad, CA, USA). Methanol and water (HPLC grade) were purchased from Merck Co. Ltd. (Darmstadt, Germany) for sample preparation and HPLC-MS/MS analysis. Ultra-pure water was obtained using a Millipore Milli-Q system (Millipore, Bedford, USA) for preparation of reagents and standard solutions.

2.2. Chromatographic conditions

Chromatographic analysis was performed on a Shimadzu HPLC system (Kyoto, Japan) equipped with system controller (DGU-20A), pump (LC-30AD), auto-injector (SIL-30AC), online degasser (DGU-20A3R), and column heater (CTO-20AC). The separations were performed using a SHIM-PACK GISS C18 column (50 mm × 2.1 mm, 1.9 μm, Shimadzu, Kyoto, Japan) with a gradient elution method. The mobile phases were (A) 0.1 % formic acid in water and (B) methanol and the method varied the solvent composition as follows: 0 min, 90 % B; 0.5 min, 90 % B; 3 min, 5 % B; 5 min, 5 % B; 5.3 min, 90 % B; 7.3 min, 90 % B. The flow rate was 0.3 ml/min. The column was heated to 40 °C and the injection volume was 5 μL.

2.3. Mass spectrometric conditions

An AB SCIEX QTRAP® 6500 tandem mass spectrometer (Framingham, MA, USA) was coupled to the HPLC system though an electrospray ionization (ESI) interface. The ESI source was operated in positive ionization mode and quantification was performed using multiple reaction monitoring (MRM) mode. High purity nitrogen (99.9 %) was used for the curtain gas (40 psi), nebulizer gas (55 psi), and heater gas (55 psi) in the mass spectrometer. The collision gas setting used for the experiment was 9 psi. The ion spray voltage was 4700 V, and the source temperature was set at 600 °C. Detection parameters for HA15 and dabrafenib (IS), including collision energy, declustering potential, and retention times are given in Table 1. Instrumental system control, data collection, and analysis were performed using AB Sciex Analyst software (version 1.6.3).

2.4. Quality control (QC) standards and calibration standards

We used 70 % (v/v) methanol aqueous solution to prepare the stock (1 mg/ml) and working solutions of HA15 and IS. All the solutions were stored at 4 °C before analysis. The standard solutions of various concentrations (2.5 ng/ml, 5 ng/ml, 10 ng/ml, 25 ng/ml, 50 ng/ml, 100 ng/ml, 200 ng/ml, 500 ng/ml, and 1000 ng/ml) for instrument calibration were prepared by diluting the HA15 stock solution in 70 % (v/v) methanol aqueous solution. A series of QC standard solutions were prepared for quantitative evaluation of the extraction recovery, matrix effect, precision, accuracy, and stability of the drug. Herein, the QC standards were prepared by spiking HA15 at low (5 ng/ml), medium (100 ng/ml) and high (500 ng/ml) concentrations into blank plasma and tissue homogenate samples.

2.5. Analytical method validation

2.5.1. Extraction recovery and matrix effect

To evaluate the extraction recovery (*Rec*) and matrix effect (*ME*) on HPLC-MS/MS quantification, QC plasma samples (50 μL each sample) were extracted with three times volumes (150 μL) of pure methanol (100 %). The values of the parameters were determined from the following equations:

$$Rec = \frac{S1}{S2} \times 100\%$$

$$ME = \frac{S2}{S3} \times 100\%$$

Where *S1* represents the peak area of of the analyte HA15 on a chromatogram of QC plasma samples after protein precipitation and analyte extraction by methanol; *S2* represents the peak area of HA15 in the extracted blank plasma samples that were spiked with HA15 with the same final concentrations as in the QC plasma samples; *S3* represents the peak area of HA15 in standard solutions.

2.5.2. Method linearity, limit of detection, and lower limit of quantification

The limit of detection (LOD) and lower limit of quantification (LLOQ) were defined as the lowest concentration yielding a signal-to-noise ratios of ≥ 3 and ≥ 10, respectively, using the analytical method. The method linearity was determined by the analysis of a series of standard solutions with different concentrations (2.5 ng/ml, 5 ng/ml, 10 ng/ml, 25 ng/ml, 50 ng/ml, 100 ng/ml, 200 ng/ml, 500 ng/ml, and 1000 ng/ml) in five replicates. HA15 concentrations were calculated using the area ratios of the transitions for HA15 to Dabrafenib (IS). A least-squares regression was used to construct the calibration curve and the correlation coefficients (r) should be ≥ 0.99.

2.5.3. Precision and accuracy

The inter- and intra-day precision were determined by analyzing the QC standards on three different days and in the same day, respectively. The precision was evaluated using the relative standard deviation (RSD) among different measurements. Accuracy is defined as the relative deviation in the measured value *(E)* of a standard from that of its true value *(T)* expressed as a percentage (Relative error, *RE* %). It was calculated by using the formula: $RE\% = (E - T)/T \times 100$. $RE\% \leq 15$ % was considered acceptable. Experiments were performed with six replicates unless otherwise specified.

2.5.4. The storage stability of plasma and tissue homogenate samples

The chemical stability of HA15 QC standards was evaluated under different storage conditions, *i.e.*, 1) -20 °C for 30 d, 2)

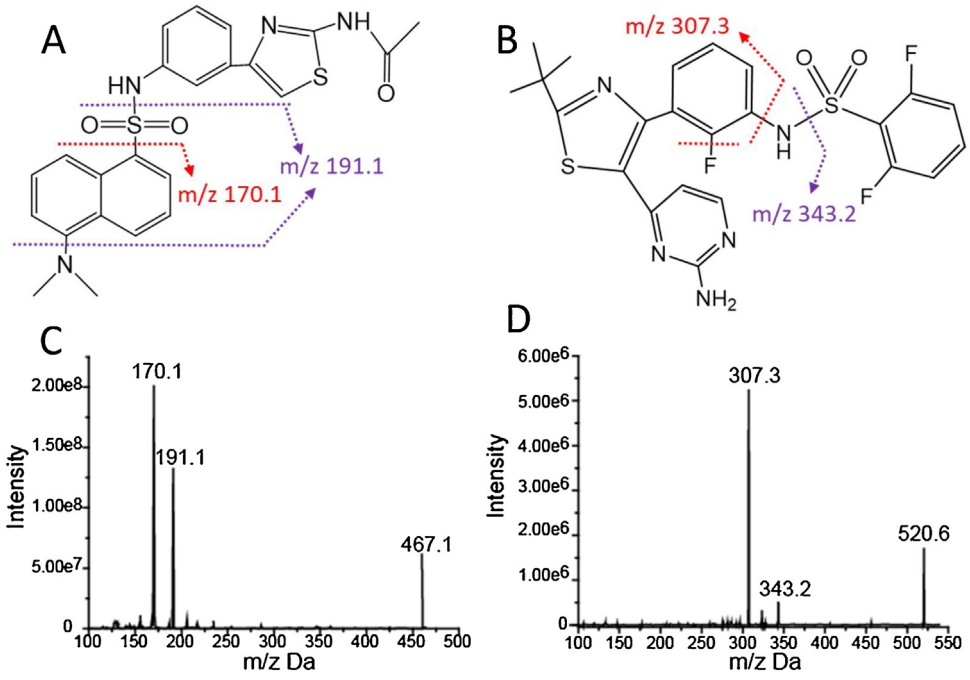

Fig. 1. The chemical structure and proposed fragmentation of (A) HA15 and (B) IS. The full-scan ion spectra of (C) HA15 and (D) IS.

three freeze-thaw cycles between -20 °C and ambient temperature, where samples were kept at each temperature for 6 h, and 3) at ambient temperature for 24 h.

2.6. MN preparation and characterization

A mixture of PVP and PVA were fabricated into MNs. Briefly, 200 mg of PVA was dissolved in 800 μl of PBS at 60 °C. HA15 solution with final concentration of 10 mg/ml in PBS was prepared. And 200 μl of the solution was dissolved in the PVA solution. Then, 500 mg of PVP powder was dispersed in the solution. Air bubbles were removed by centrifugation at 8000 rpm for 5 min. The polymer mixture was fabricated into MNs through the following steps: (a) MN molds made from PDMS were treated with an O_2 plasma cleaner (Mingheng Science and Technology Development Co., Ltd., Chengdu, China) for 20 s to increase the hydrophilicity of the microvoids; (b) 30 μl of HA15-loaded polymer solution was added to fill the microvoids, and excess solution was removed from the mold surface with a flat blade; (c) the solution was dried at 40 °C for 1 h to allow them to form the MN tips; (d) 100 μl of HA15-free polymer solution was then cast onto the mold and dried at 40 °C for 10 h; (e) the MNs were gently peeled from the mold by using adhesive tape. The MN patches were stored in a desiccator until use. To study the MN morphology, they were sputter-coated with 8 nm of platinum using a Leica SCD500 cryo sputter coater (Leica Microsystems, Vienna, Austria) for 30 s. Afterwards, the microneedles were imaged using a ZEISS SUPRA 55 scanning electron microscope (SEM; Carl Zeiss, Oberkochen, Germany).

2.7. HA15 loading and dissolution from MNs

During MN patch fabrication, 50 μg of HA15 was loaded into each MN patch. However, it is still important to measure the real drug loading amount so as to know if there is drug loss during fabrication. For this purpose, the MN Patch was first dissolved in 2 ml of water, and then 6 ml of methanol was added and vortexed for 5 min. After centrifuging at 12,000 rpm for 10 min, 500 μl of the supernatant was transferred to a new tube to mix with 500 μl IS solution. The mixture solution was filtered with 0.22 μm membrane syringe filters and analyzed with the developed HPLC-MS/MS for HA15 quantitation. Similarly, the HA15 release kinetics was studied. Herein, first the HA15-loaded MNs were incubated in a beaker containing 5 ml DI water at room temperature. At each predetermined time-point (2 min, 4 min, 6 min, 8 min, and 10 min), 100 μl of the dissolution medium was removed and the sample was replenished with the same amount of DI water. Then 300 μl methanol was added into the collected dissolution medium and vortexed for 5 min. After centrifuging at 12,000 rpm for 10 min, the supernatant was transferred to a new tube and mixed with 400 μl IS solution, prior to filtration and HPLC-MS/MS analysis.

2.8. In vitro *transdermal efficiency*

The HA15 transdermal delivery efficiency was evaluated by using a vertical Franz diffusion cell system (TP-6, Tianguang Photoelectric Instrument Co., Tianjin, China). Isolated mouse skins were carefully shaved and washed with PBS twice. HA15 loaded MN patches were applied to the skin by pressing them down with a thumb for 10 s and leaving them embedded for another 20 min to

Table 1
Optimized conditions for quantification of HA15 and Dabrafenib (IS) using HPLC-MS/MS.

Analyte	MRM transition (*m/z*)	Ions	Collision energy (eV)	Decluster potential (V)	Retention time (min)
HA15	467.1→170.1	quantifier	32	90	3.7
	467.1→191.1	qualifier	35	95	3.7
Dabrafenib (IS)	520.6→307.3	quantifier	32	90	3.7
	520.6→343.2	qualifier	35	95	3.7

dissolve. Afterwards, the MN patches were removed, and the skins were placed onto the Franz cells with their dermal sides facing the receptor chamber and the MN treatment areas at the center of the cell. The permeation area of Franz cell was ~1.77 cm^2 d =1.5 cm. The receptor chamber was filled with PBS solution 20 ml, pH 7.4. Care was taken to avoid forming air bubbles below the skin tissue. The experiment was performed at 37 °C in a water bath incubator with continuous stirring at 600 rpm. At 2, 4, 6, 8, 10, 22, 34, 46, 58, 72 h after MN application, 1 ml of the solution in each receptor chamber was collected and replaced with an equal volume of PBS buffer. The collected receptor solution was mixed with 3 ml of methanol, vortexed for 5 min, and then centrifuged at 12,000 rpm for 5 min. Afterwards, 500 μl of the supernatant were transferred to a new tube and mixed with 500 μl IS solution, prior to filtration and HPLC-MS/MS analysis.

2.9. Cell culture

B16F10 cells were cultured in DMEM medium supplemented with 10 % FBS, 100 μg/ml of penicillin, and 100 μg/ml of streptomycin. The cells were cultured at 37 °C in an atmosphere of 5% CO_2 and passaged every 2 d.

2.10. *HA15* in vivo *antitumor assay*

All of the animal studies were performed in the laboratory animal center, Cancer Hospital, Chinese Academy of Medical Sciences, Shenzhen Center. The experimental procedures were based on the guidelines on animal care and use of Principles of Laboratory Animal Care (NIH publication no. 86-23, revised 1985) and approved by the institutional animal care committee at the Cancer Hospital, Chinese Academy of Medical Sciences, Shenzhen Center (No. NCC2019A005).

Female BALB/c-nu/nu mice 11–13 g, 21–28 days were supplied by the Southern Medical School Laboratory Animal Center No. 44002100020555. When their body weight reached 15–18 g, they were used to evaluate the antitumor efficacy of HA15 MNs *in vivo*. In detail, 100 μl of B16F10 cells with a concentration of 5×10^6 cells/ml were subcutaneously injected into the left flank of the mice. When the tumor volumes grew to 70–100 mm^3, the mice were randomly divided into three groups (with six mice per group): 1) the saline group, where the mice were subcutaneously injected with 0.1 ml of saline solution near the tumor sites; 2) the HA15 MNs group, where the mice were treated with HA15-loaded MNs ~1.5 cm distant from the tumor sites (each MN patch was inserted into the skin with thumb pressure for 5 min and left in place for 20 min before removing); and 3) the subcutaneous (SC) injection group, where the mice were injected with 0.1 ml of HA15 solution (50 μg/mouse). On day 12, the mice in each group were sacrificed for further analysis.

2.11. Plasma sample preparation

Blood was collected from the eyes of each mouse at 1, 3, and 12 h after DPMN or subcutaneous administration. The blood was stored at 4 °C overnight before centrifuging at 3000 rpm for 20 min to separate the plasma. The plasma was stored at -80 °C and they were thawed at ambient temperature before analysis. Each plasma sample (50 μL) was mixed with 150 μL methanol in a 1.5 ml Eppendorf tube, and vortexed for 5 min to precipitate proteins. After centrifuging at 12,000 rpm for 10 min, the supernatant was mixed with 200 μl IS solution for filtration and HPLC-MS/MS analysis.

2.12. Tissue sample preparation

At three time-points, *i.e.*, 1, 3, and 12 h after DPMN or subcutaneous administration, the main organs (the livers, kidneys, hearts, spleens, and lungs) were removed from the sacrificed mice, washed and dried at ambient temperature. They were cut into small pieces using ophthalmic scissors and weighed; then 0.1 g of each tissue sample was placed in 96-well plates. Afterwards, 150 μl methanol and 50 μl DI water were added in each sample and mixed before they were transferred to new 1.5 ml Eppendorf tubes. The tissue homogenate samples were prepared by ultrasonic cell crusher Sonics Vibra-Cell; Sonics & Materials, Inc., Newtown, CT, USA on ice, which ultrasonic 10 s, intermittent 5 s, and repeated 6 times. The samples were then centrifuged at 12,000 rpm for 20 min. The supernatants were collected and stored at -80 °C until use. Before LC–MS/MS detection, they were mixed with the IS solution before filtration.

2.13. Statistical analysis

Results are presented as the mean of the replicates and associated standard deviations. Statistical difference values were determined using SPSS 24.0 for Windows software (IBM, Istanbul, Turkey) using Student's t-test. Differences were considered as statistically significant when $p < 0.05$.

3. Results and discussion

3.1. Method development

All of the operation parameters were carefully optimized for the determination of HA15 and the IS. Analyses yielded higher intensities in positive ion than in negative ion mode. As shown in Table 1 and Fig. 1, two MRM transitions were used to confirm the analyte identification [25,26]. Under positive ion electrospray ionization (ES^+), HA15 forms a molecular ion of mass-to-charge ratio (*m/z*) 467.1 Da and two major daughter ions at *m/z* 170.1 and 191.1 Da, which were used as quantifier and qualifier ions, respectively. Likewise, IS generated a molecular ion *m/z* at 520.6 Da, and two major daughter ions at *m/z* 307.3 and 343.2 Da. The transition 520.6→307.3 was used for quantification and the transition 520.6→343.2 was used for qualification.

The chromatographic conditions were optimized for the resolution and specificity of analyte peaks. Methanol was chosen as the mobile phase because HA15 and IS yield higher signals than when using acetonitrile [27]. 0.1 vol% formic acid significantly increased the sensitivity toward HA15 and IS. Gradient elution minimized analysis time while retaining good resolution. We assessed solid phase (C18 SPE) and liquid phase extraction techniques, however, using methanol/H_2O (3:1 v/v) as the protein precipitation solvent resulted in satisfactory recovery, matrix effects, and reproducibility for HA15 quantification and was considerably more simple, sensitive, and rapid than using an SPE column. Because a stable isotopically labeled analog of HA15 was unavailable, dabrafenib, a similar sulfonamide with similar retention as HA15 in the present assay (Table 1, Fig. S1), was selected as the internal standard to correct for any analyte loss during instrumental analysis.

Both transitions for the analyte HA15 and the IS were employed for quantification of analyte in QC standard solutions (Fig. S2) generating the same results, validating the analytical method.

3.2. Method validation

3.2.1. Selectivity, extraction recovery, and matrix effect

Plasma blank samples (without spiked analyte) were prepared and injected into the HPLC-MS/MS instrument to evaluate the

Table 2
Precision and accuracy of the HA15 LC–MS/MS detection method (n=6 for 3 d).

[HA15] (ng ml^{-1})	Inter-day			Intra-day		
	Measured [HA15] (ng ml^{-1})	Precision (%, RSD)	Accuracy (%, RE)	Measured [HA15] (ng ml^{-1})	Precision (%, RSD)	Accuracy (%, RE)
5	5.54 ± 0.18	3.06	9.69	5.29 ± 0.41	7.68	5.45
100	105.33 ± 4.85	4.61	5.07	98.64 ± 7.32	7.42	−1.38
500	500.91 ± 1.83	0.37	0.18	500.13 ± 2.49	0.50	0.03

Table 3
Stability of HA15 under different storage conditions in plasma and in organ samples (n=5).

[HA15] (ng ml^{-1})	Plasma stability (mean ± SD)			Tissue homogenate stability (mean ± SD)		
	Long-term	Freeze-thaw	Ambient temperature	Long-term	Freeze-thaw	Ambient temperature
5	4.80 ± 0.25	4.92 ± 0.18	4.89 ± 0.09	4.78 ± 0.33	4.69 ± 0.33	4.90 ± 0.05
100	99.07 ± 7.99	100.76 ± 4.05	100.79 ± 4.27	98.57 ± 10.49	99.19 ± 8.19	97.13 ± 7.01
500	478.45 ± 33.99	482.19 ± 19.45	471.29 ± 13.50	490.01 ± 10.45	472.05 ± 20.33	461.11 ± 28.15

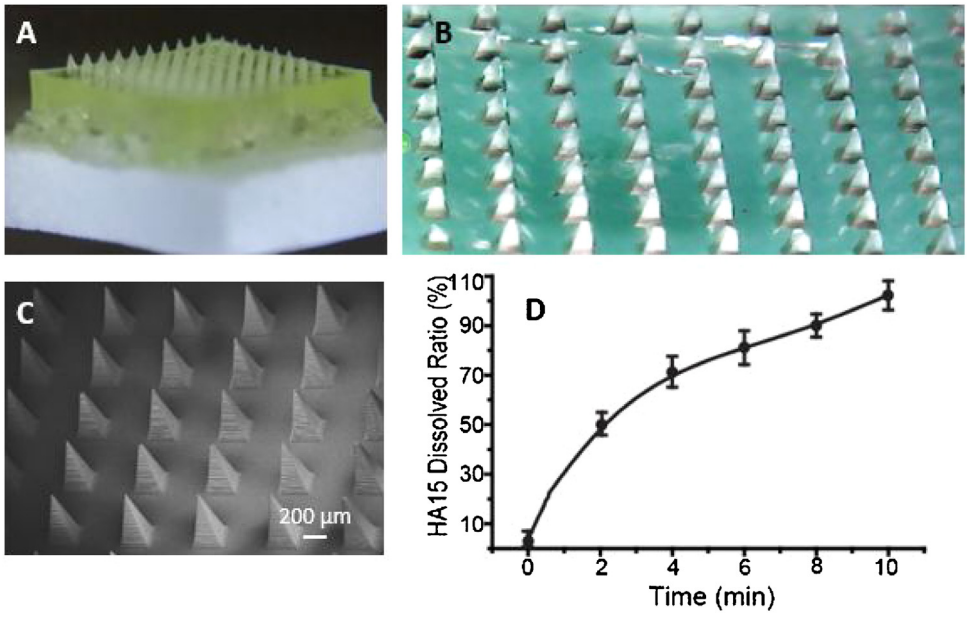

Fig. 2. (A) Digital and (B) magnified images of the HA15 DPMNs. (C) An SEM image of the DPMNs at 30 times direct magnification. (D) Dissolution profiles of HA15 from DPMNs in water.

selectivity of the method. Herein, there were no chromatographic interferences that co-elute with HA15 (Fig. S3A) or the IS (Fig. S3B). The QC standards were used for the extraction recovery and matrix effect determination. The mean extraction recovery ratio of HA15 at the three concentrations, *i.e.*, 5, 100, 500 ng/ml, were 90.2, 95.2, and 94.3 % with RSD values of 9.6 %, 8.0 %, and 3.6 %, respectively. Additionally, for evaluating the matrix effect, the % recoveries of the drug HA15 on the three concentrations were 85.3, 89.2, and 94.3 %, respectively, demonstrating that there was no significant matrix effect (p > 0.05) on HA15 quantification.

3.2.2. Linearity, LOD, and LLOQ

Linear calibration curves were obtained by plotting the peak area ratio (y) of HA15: IS versus the HA15 concentration. A weighted (1/x) least-squares regression analysis yielded the linear equation: $y = 53205\,x + 822198$ ($r = 0.99877$). Good linearity was exhibited over the concentration range 2.5–1000 ng/ml. The LLOQ and LOD were 2.5 and 1 ng/ml, respectively.

3.2.3. Precision and accuracy

The method performance data for HA15 evaluated using the QC samples are reported in Table 2. Inter- and intra-day RSD and RE values were <7.7 % and <5.5 %, respectively. Therefore, the precision and accuracy were acceptable (within ±15 % variation).

3.2.4. Sample stability in plasma and tissue homogenate samples

Table 3 summarizes the stability, *i.e.*, long-term, freeze-thaw, and ambient temperature, of HA15 in plasma and tissue homogenates. The results indicate that HA15 is stable under the storage conditions described above because there was no significant difference between the measured concentrations of HA15 and its dosed concentrations (p > 0.05).

3.3. HA15 loading and dissolution from DPMNs in vitro

PVP and PVA were selected for DPMN fabrication because of their biocompatibility and water solubility. PVP is a rapidly dissolvable polymer but it is soft and moisture sensitive. PVA was therefore added to enhance stiffness and stability. A two-step casting procedure was used to generate HA15 loaded tips with drug-free bodies. As shown in Fig. 2A, 10 × 10 highly uniform DPMN arrays with area ~1.5 cm^2 were fabricated. The microneedles had 350, 700, and ~15 µm bases, heights, and tip widths, respectively, with 500 µm needle center-to-center spacing (Figs. 2B and C).

Ten DPMNs were dissolved in water and the drug was extracted for LC–MS/MS analysis, which showed an HA15 content of 49.70 ± 3.25 μg, demonstrating reproducible drug loading. Additionally, we investigated the *in vitro* HA15 DPMN dissolution kinetics, with ~50 % dissolution in 5 min and complete dissolution in 10 min, which was slightly slower than similar PVP DPMNs [17,20].

3.4. Ex vivo *DPMN skin insertion and drug delivery*

DPMNs require high mechanical strength to penetrate the *stratum corneum* during drug delivery. The prepared DPMNs were applied to mouse skin *ex vivo* by applying thumb pressure on their backside. After insertion into the skin, almost all of the microneedles (10 × 10) were dissolved (Fig. 3A), and a complete array of violet spots (10 × 10) indicated that all the microneedles were successfully inserted into the skin (Fig. 3B).

The treated skins were transferred to a Franz diffusion cell system to evaluate the transdermal efficiency of HA15 *ex vivo*. As shown in Fig. 3C, the amount of HA15 delivered through the skin was 5% after 24 h, which slowly increased to 18 % after 48 h. The transdermal delivery then increased rapidly between 48–72 h to 51 %. After 72 h, the skins were removed and HA15 was extracted for quantification. The results showed 39.01 % remained within skins (RSD 3.36 %), leaving only about 10 % unaccounted for, either within the skin or lost during the sample preparation. This data suggested that first, HA15 did not diffuse up into the base of the microneedle patch during the fabricated process, and second, HA15 insertion into the skin was with high efficiency (>90 %) with no significant amount of HA15 loss during the skin insertion.

3.5. Tissue distribution of HA15 in BALB/c-nu/nu mice

The validated analysis method was applied to tissue homogenates obtained from the B16F10 tumor-bearing BALB/c-nu/nu mice that received control or HA15 treatments given through DPMNs or SC administration (50 μg/mouse). The liver, heart, spleen, lung, kidney, tumor, and plasma concentrations of HA15 1, 3, and 12 h after treatment are presented in Fig. 4. Mice receiving SC administration obtained the highest tissue HA15 concentration levels after 1 h, except for the kidney, which achieved a higher level after 3 h. SC administration resulted in rapid metabolism such that no drug was detected in the tumor site, or any other tissue with the exception of the spleen, after 12 h. Although a high concentration of HA15 (425 ng/g) was measured at the tumor site within 1 h, more was measured in the kidney (775 ng/g) and liver (1563 ng/g), suggesting the potential for side effects in these organs. However, MN administration presented a different distribution profile. The concentration was low in all of the organs because of the slow and prolonged drug release of the DPMNs, with consistent measurements over the first 12 h, *e.g.*, Fig. 4F, the tumor site, has 75, 65, and 75 ng/g of HA15 after 1, 3, and 12 h, respectively. However, HA15 may release more quickly after 48 h, as seen in the *ex vivo* transdermal assay. The drug did not accumulate in the liver and kidney. Although the highest liver tissue concentration was achieved in 1 h, it was only 1.3–1.7 times higher than in tumor site after 12 h whereas the

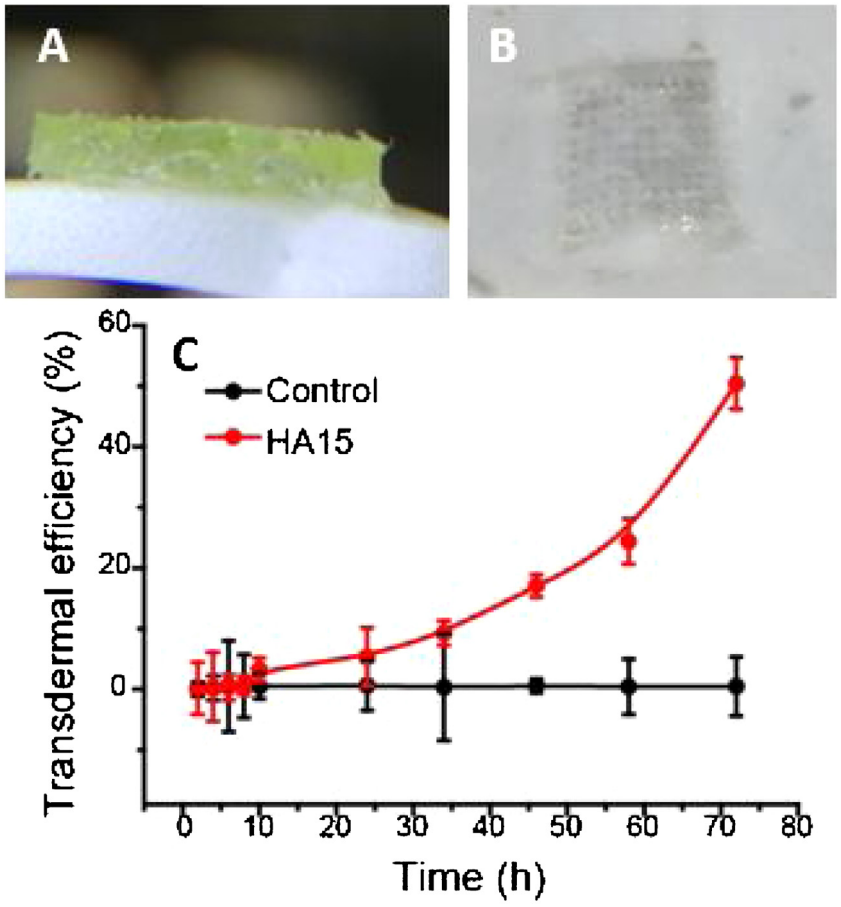

Fig. 3. (A) A digital image of a microneedle patch after skin insertion for 20 min, of which all the microneedles were inserted and dissolved within the skin tissue. (B) A digital image of mouse skin *ex vivo* after applying a 10 × 10 DPMN array. (C) The transdermal efficiency-time profile of HA15 DPMNs in mouse skin *ex vivo*.

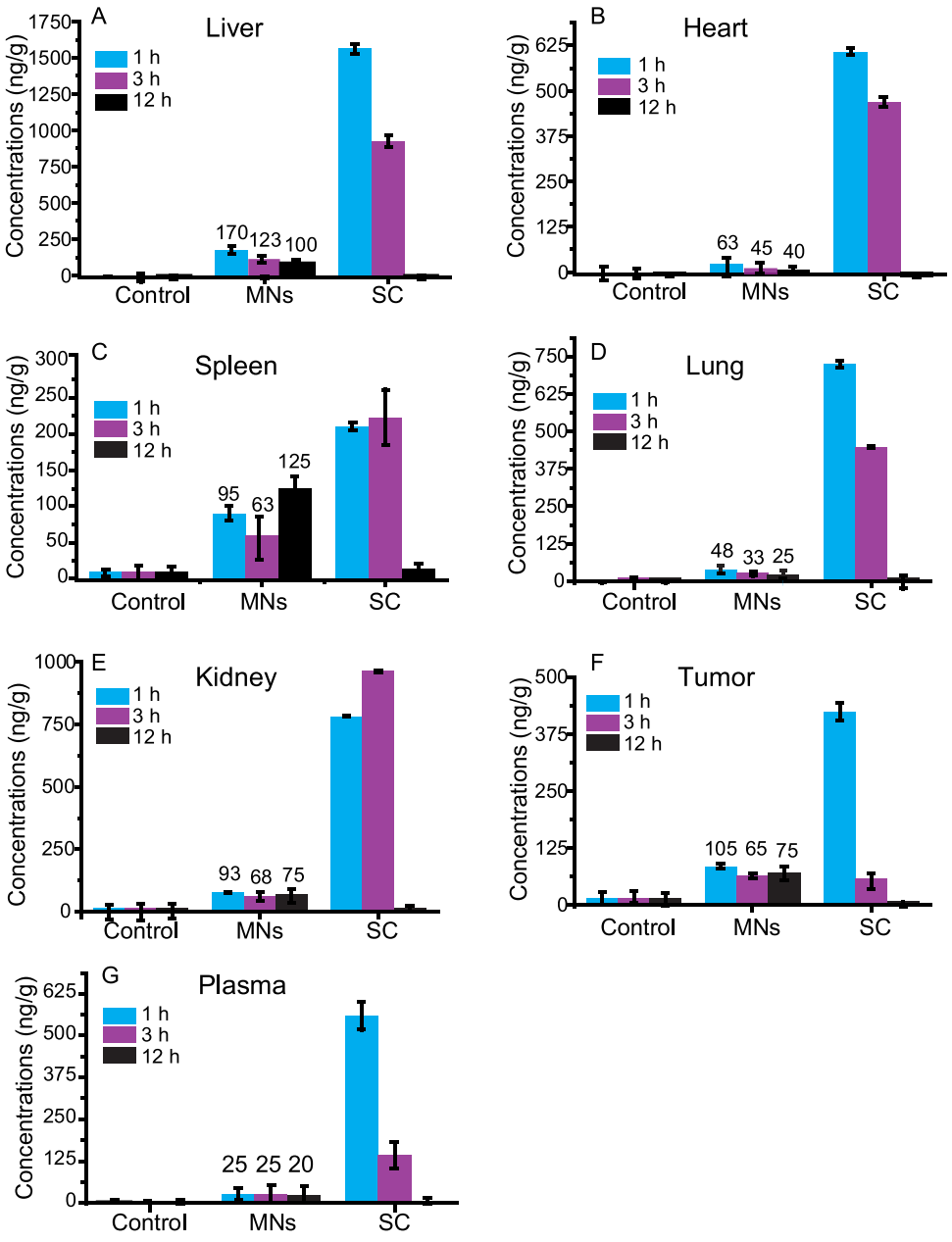

Fig. 4. The concentration of HA15 in the (A) liver, (B) heart, (C) spleen, (D) lung, (E) kidney, (F) tumor, and (G) plasma after DPMN and SC administration in tumor-bearing nude mice.

kidney was very similar to the tumor site. These data suggest that DPMN administration might have fewer side effects in the liver and kidney. Altogether, the tissue distribution data provides considerable evidence for the slower drug release profile and drug accumulation changes for MN treatments.

4. Conclusions

A validated assay for the sensitive and reliable determination of HA15 in bio-samples has been fully developed using LC–MS/MS. The sensitive assay includes a fast and simple sample extraction with high recovery (>90 %). In addition, the results show values for the matrix effect, LOD, LLOQ, linear range, accuracy, precision, and stability required by international guidelines [28,29]. The assay was successfully applied to investigate the drug loading, drug dissolution kinetics, and *ex vivo* transdermal release performance of HA15 in DPMNs. Moreover, the systemic comparison of the distribution in plasma, major organs, and tumors by DPMN and SC administration were investigated. The results showed a relatively slower and stable release of HA15 by DPMNs, which did not accumulate the drug in the liver and kidney, and which might reduce side effects. Altogether, this study developed a validated method for HA15 determination and provided a valuable evidence of its bio-distribution for transdermal delivery systems development.

Compliance with ethical standards

All the animal experiments in the present study were approved by the Ethical Committee of Cancer Hospital, Chinese Academy of Medical Sciences, Shenzhen Center (NCC2019A005).

CRediT authorship contribution statement

Parbeen Singh: Methodology, Investigation, Data curation, Funding acquisition. **Xiliu Zeng:** Methodology, Investigation, Validation, Software. **Xiaowu Chen:** Methodology, Validation. **Yikun Yang:** Methodology, Resources. **Yongli Chen:** Conceptualization, Data curation, Formal analysis, Writing - original draft, Funding acquisition. **Shufen Cui:** Resources, Supervision, Funding acquisition. **Andrew Carrier:** Methodology, Writing - review & editing. **Ken Oakes:** Supervision, Project administration. **Tiangang Luan:** Visualization, Project administration. **Xu Zhang:** Conceptualization, Writing - review & editing, Funding acquisition.

Declaration of Competing Interest

The authors declare that they have no conflict of interest.

Acknowledgements

This work was supported by the Beatrice Hunter Cancer Research Institute (BHCRI), China Postdoctoral Science Foundation (2019M653139, 2019M653979), Guangdong Province Higher Vocational College & School's Pearl River Scholar Funded Scheme (2017), Canada Research Chairs program, New Frontiers in Research Fund - Exploration (NFRFE-2018-01005), the Scientific and Technological Foundation of Shenzhen, China (No. GJHZ20180928161212140). Atlantic Canada Opportunities Agency AIF program, Cape Breton University RISE program, NSERC Discovery Grants Program, and Post-doctoral Foundation Project of Shenzhen Polytechnic (6019330001K, 6019330006K, 6019330007K).

Appendix A. Supplementary data

Supplementary material related to this article can be found, in the online version, at doi:https://doi.org/10.1016/j.jpba.2020.113230.

References

[1] M. Cerezo, A. Lehraiki, A. Millet, F. Rouaud, M. Plaisant, E. Jaune, T. Botton, C. Ronco, P. Abbe, H. Amdouni, T. Passeron, V. Hofman, B. Mograbi, A.S. Dabert-Gay, D. Debayle, D. Alcor, N. Rabhi, J.S. Annicotte, L. Heliot, M. Gonzalez-Pisfil, C. Robert, S. Morera, A. Vigouroux, P. Gual, M.M.U. Ali, C. Bertolotto, P. Hofman, R. Ballotti, R. Benhida, S. Rocchi, Compounds triggering ER stress exert anti-melanoma effects and overcome BRAF inhibitor resistance, Cancer Cell 29 (2016) 805–819.
[2] C. Ruggiero, M. Doghman-Bouguerra, C. Ronco, R. Benhida, S. Rocchi, E. Lalli, The GRP78/BiP inhibitor HA15 synergizes with mitotane action against adrenocortical carcinoma cells through convergent activation of ER stress pathways, Mol. Cell. Endocrinol. 474 (2018) 57–64.
[3] M. Cerezo, S. Rocchi, New anti-cancer molecules targeting HSPA5/BIP to induce endoplasmic reticulum stress, autophagy and apoptosis, Autophagy 13 (2017) 216–217.
[4] J. McLenon, M.A.M. Rogers, The fear of needles: a systematic review and meta-analysis, J. Adv. Nurs. 75 (1) (2019) 30–42.
[5] Y.J.F. Hutin, R.T. Chen, Injection safety: a global challenge, Bull. World Health Organ. 77 (10) (1999) 787–788.
[6] S. Henry, D.V. McAllister, M.G. Allen, M.R. Prausnitz, Microfabricated microneedles: a novel approach to transdermal drug delivery, J. Pharm. Sci. 87 (1998) 922–925.
[7] M.R. Prausnitz, R. Langer, Transdermal drug delivery, Nat. Biotech. 26 (2008) 1261–1268.
[8] R.F. Donnelly, T.R. Singh, M.J. Garland, K. Migalska, R. Majithiya, C.M. McCrudden, P.L. Kole, T.M. Mahmood, H.O. McCarthy, A.D. Woolfson, Hydrogel-forming microneedle arrays for enhanced transdermal drug delivery, Adv. Funct. Mater. 22 (2012) 4879–4890.
[9] T. Waghule, G. Singhvi, S.K. Dubey, M.M. Pandey, G. Gupta, M. Singh, K. Dua, Microneedles: a smart approach and increasing potential for transdermal drug delivery system, Biomed. Pharmacother. 109 (2019) 1249–1258.
[10] E. Larraneta, M.T. McCrudden, A.J. Courtenay, R.F. Donnelly, Microneedles: a new frontier in nanomedicine delivery, Pharm. Res. 33 (2016) 1055–1073.
[11] W. Huang, D. Restrepo, J.Y. Jung, F.Y. Su, Z. Liu, R.O. Ritchie, J. McKittrick, P. Zavattieri, D. Kisailus, Multiscale toughening mechanisms in biological materials and bioinspired designs, Adv. Mater. 31 (2019), e1901561.
[12] P. Singh, A. Carrier, Y. Chen, S. Lin, J. Wang, S. Cui, X. Zhang, Polymeric microneedles for controlled transdermal drug delivery, J. Control. Release 315 (2019) 97–113.
[13] C. Chiappini, E. De Rosa, J.O. Martinez, X. Liu, J. Steele, M.M. Stevens, E. Tasciotti, Biodegradable silicon nanoneedles delivering nucleic acids intracellularly induce localized in vivo neovascularization, Nat. Mater. 14 (2015) 532–539.
[14] H. Chen, B. Wu, M. Zhang, P. Yang, B. Yang, W. Qin, Q. Wang, X. Wen, M. Chen, G. Quan, X. Pan, C. Wu, A novel scalable fabrication process for the production of dissolving microneedle arrays, Drug Deliv. Transl. Res. 9 (1) (2019) 240–248.
[15] J.W. Lee, J.-H. Park, M.R. Prausnitz, Dissolving microneedles for transdermal drug delivery, Biomaterials 29 (13) (2008) 2113–2124.
[16] N.G. Rouphael, M. Paine, R. Mosley, S. Henry, D.V. McAllister, H. Kalluri, W. Pewin, P.M. Frew, T. Yu, N.J. Thornburg, S. Kabbani, L. Lai, E.V. Vassilieva, I. Skountzou, R.W. Compans, M.J. Mulligan, M.R. Prausnitz, A. Beck, S. Edupuganti, S. Heeke, C. Kelley, W. Nesheim, The safety, immunogenicity, and acceptability of inactivated influenza vaccine delivered by microneedle patch (TIV-MNP 2015): a randomised, partly blinded, placebo-controlled, phase 1 trial, Lancet 390 (10095) (2017) 649–658.
[17] S.P. Sullivan, N. Murthy, M.R. Prausnitz, Minimally invasive protein delivery with rapidly dissolving polymer microneedles, Adv. Mater. 20 (5) (2008) 933–938.
[18] W. Li, R.N. Terry, J. Tang, M.R. Feng, S.P. Schwendeman, M.R. Prausnitz, Rapidly separable microneedle patch for the sustained release of a contraceptive, Nat. Biomed. Eng. 3 (2019) 220–229.
[19] Y. Chen, Y. Yang, Y. Xian, P. Singh, J. Feng, S. Cui, A. Carrier, K. Oakes, T. Luan, X. Zhang, Multifunctional graphene-oxide-Reinforced dissolvable polymeric microneedles for transdermal drug delivery, ACS Appl. Mater. Inter. 12 (1) (2019) 352–360.
[20] C. Tas, J.C. Joyce, H.X. Nguyen, P. Eangoor, J.S. Knaack, A.K. Banga, M.R. Prausnitz, Dihydroergotamine mesylate-loaded dissolving microneedle patch made of polyvinylpyrrolidone for management of acute migraine therapy, J. Control. Release 268 (2017) 159–165.
[21] Z. Zhu, H. Luo, W. Lu, H. Luan, Y. Wu, J. Luo, Y. Wang, J. Pi, C.Y. Lim, H. Wang, Rapidly dissolvable microneedle patches for transdermal delivery of exenatide, Pharm. Res. 31 (2014) 3348–3360.
[22] H.R. Jeong, J.Y. Kim, S.N. Kim, J.H. Park, Local dermal delivery of cyclosporin A, a hydrophobic and high molecular weight drug, using dissolving microneedles, Eur. J. Pharm. Biopharm. 127 (2018) 237–243.
[23] M.N. Kelchen, N.K. Brogden, In vitro skin retention and drug permeation through intact and microneedle pretreated skin after application of propranolol loaded microemulsions, Pharm. Res. 35 (2018) 228.
[24] C. Dillon, H. Hughes, N.J. O'Reilly, C.J. Allender, D.A. Barrow, P. McLoughlin, Dissolving microneedle based transdermal delivery of therapeutic peptide analogues, Int. J. Pharm. 565 (2019) 9–19.
[25] A.A. Okhina, A.D. Rogachev, O.I. Yarovaya, M.V. Khvostov, T.G. Tolstikova, A.G. Pokrovsky, V.A. Khazanov, N.F. Salakhutdinov, Development and validation of an LC-MS/MS method for the quantitative analysis of the anti-influenza agent camphecene in rat plasma and its application to study the blood-to-plasma distribution of the agent, J. Pharm. Biomed. Anal. 180 (2020), 113039.
[26] J.P. Pascali, P. Fais, F. Vaiano, N. Pigaiani, S. D'Errico, S. Furlanetto, D. Palumbo, E. Bertol, Internet pseudoscience: testing opioid containing formulations with tampering potential, J. Pharm. Biomed. Anal. 153 (2018) 16–21.
[27] R.W. Sparidans, S. Durmus, A.H. Schinkel, J.H. Schellens, J.H. Beijnen, Liquid chromatography-tandem mass spectrometric assay for the mutated BRAF inhibitor dabrafenib in mouse plasma, J. Chromatogr. B 925 (2013) 124–128.
[28] O. González, M.E. Blanco, G. Iriarte, L. Bartolomé, M.I. Maguregui, R.M. Alonso, Bioanalytical chromatographic method validation according to current regulations, with a special focus on the non-well defined parameters limit of quantification, robustness and matrix effect, J. Chromatogr. A 1353 (2014) 10–27.
[29] S. Kollipara, G. Bende, N. Agarwal, B. Varshney, J. Paliwal, International guidelines for bioanalytical method validation: a comparison and discussion on current scenario, Chromatographia 73 (3) (2011) 201–217.